Journal of Hazardous Materials 194 (2011) 92–99

Contents lists available at ScienceDirect

Journal of Hazardous Materials

journal homepage: www.elsevier.com/locate/jhazmat

Removal of Cu(II) and Cr(VI) ions from aqueous solution using chelating fiber packed column: Equilibrium and kinetic studies

Young Gun Ko[a], Yong Jin Chun[b], Choong Hyun Kim[a], Ung Su Choi[a,*]

[a] Energy Mechanics Center, Korea Institute of Science and Technology, 39-1 Hawolgok-dong, Wolsong-gil 5, Seongbuk-gu, Seoul 136-791, Republic of Korea
[b] Department of Materials Science and Applied Chemistry, Chungwoon University, San 29, Namjang, Hongsung, Chungnam 350-701, Republic of Korea

ARTICLE INFO

Article history:
Received 13 April 2011
Received in revised form 20 July 2011
Accepted 21 July 2011
Available online 5 August 2011

Keywords:
Chelating fiber
Heavy metal ions
Adsorption
Amine group
Crystal growth of metal ions

ABSTRACT

Herein, we demonstrate the adsorption process system with the diethylenetriamne coupled polyacrylonitrile fiber for the removal of Cu(II) and Cr(VI) ions in the aqueous solution. The synthesized chelating fiber showed a high adsorption capacity of 11.4 mequiv/g. Interestingly, the crystal growth of copper ions on the chelating fiber was observed during the adsorption process. The chelating fiber packed column showed the high performance of the removal of Cu(II) in the aqueous solution due to the distinct characteristic of the crystal growth of metal ions on the chelating fiber. After Cu(II) adsorption on the chelating fiber, the color of the fiber changed to light blue from yellow. The isotherm parameter n of 1.991 was obtained with Freundlich isotherm model for the adsorption equilibrium study which indicates that Cu(II) adsorption on the chelating fiber is very favorable due to $n > 1$. The pseudo-first-order and pseudo-second-order model equations were used for the kinetic study.

1. Introduction

Heavy metals are significant environmental pollutants, and their toxicity is a problem of increasing significance for ecological, evolutionary, nutritional and environmental reasons. Industrial effluents discharged from electroplating, mining, extracting, and printing units contain heavy metal ions at high concentrations, including high levels of Cu(II) and Cr(VI) [1]. Some heavy metals, such as copper, are known to be essential to life; however, when they exceed a certain threshold value, they can cause detrimental and acute effects [2]. Copper induces oxidative stress and DNA damage in bacteria, algae, yeasts, mice, and human cells [3]. Chromium can exist in the form of several oxidation states, however, from the environmental point of view only the trivalent and hexavalent forms are important. Cr(VI) can be toxic as it can diffuse as CrO_4^{2-} or $HCrO_4^-$ through cell membranes and oxidize biological molecules [4].

The amount of heavy metals in wastewater should be minimized to prevent accumulation in the biosphere. Many physicochemical treatment processes have been developed to remove heavy metal ions from industrial effluents, these include reverse osmosis, ion exchange, electrodialysis, evaporation, chemical precipitation, flocculation, membrane separation and chelation. Most often, these methods have a high cost, generate secondary pollutants or are simply inefficient, especially in removing toxic metal ions in trace quantities from solution [5]. Of all the various methods, adsorption using low-cost adsorbents is considered to be an economical and effective method for removal of heavy metals from aqueous solutions [6]. There are many types of adsorbents, including activated carbon fibers [7], oxide minerals [8], resins [9], and biosorbents [10]. Chelate materials are critically effective adsorbents [11–16]. Generally, the chelate materials that are used are resin beads [17]. However, fibrous chelate materials have several advantages over conventional chelate beads; for example, they are easier to prepare. Other advantages include the ability to be fabricated as felts of fabrics, which display greatly improved contact efficiencies with the media. This enhanced availability of the substrate should enhance both reaction and regeneration rates [18,19].

In our previous work, diethylenetriamine (DETA) was successfully incorporated into polyacrylonitrile (PAN) fiber to synthesize a chelating fiber with high performance [20]. This study focuses on the adsorption process of Cu(II) and Cr(VI) from the aqueous system with a chelating fiber packed column. Cu^{2+} and CrO_4^{2-} were used as a cation and an anion for the Cu(II) and Cr(VI) adsorption tests. The general ion exchanger shows the limit of adsorption capacity because metal ions adsorbed on it as a monolayer. The crystal growth of metal ions on absorbents is the key to increase the adsorption capacity. In this study, the surface of the chelating fiber packed in a column was observed with a field emission scanning electron microscopy (FE-SEM) after the adsorption process. The synthesis of the chelating fiber was confirmed with a Fourier transform infrared (FT-IR) spectroscopy and a ^{13}C solid state nuclear magnetic resonance (NMR) spectroscopy.

* Corresponding author. Tel.: +82 2 958 5657; fax: +82 2 958 5659.
E-mail address: uschoi@kist.re.kr (U.S. Choi).

0304-3894/$ – see front matter © 2011 Elsevier B.V. All rights reserved.
doi:10.1016/j.jhazmat.2011.07.088

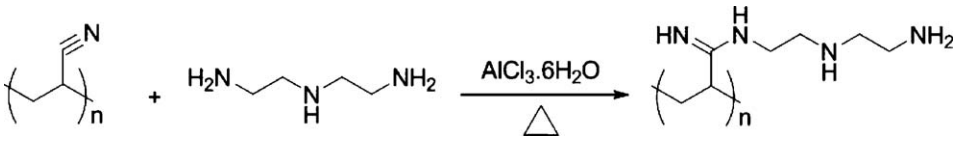

Fig. 1. Synthesis scheme of poly(acrylo-amidino diethylenediamine) (PADD).

This article reports breakthrough studies on Cu(II) and Cr(VI) removal from aqueous solutions using DETA coupled PAN fiber packed columns at the laboratory scale with varying concentration of metal ions and adsorption times as well as equilibrium and kinetic modeling of the data.

2. Experimental

2.1. Synthesis of poly(acrylo-amidino diethylenediamine) (PADD)

Polyacrylonitrile (PAN) fiber was provided from Hanil Synthetic Fiber Co., Ltd. (Korea). The fiber was extracted with ethanol and agitation for 1 day at room temperature for the removal of impurities, and it was dried *in vacuo*. Diethylenetriamine (DETA, Acros Organics Co.) was also dried at 40 °C *in vacuo* before the use. Poly(acrylo-amidino diethylenediamine) was obtained through the heating of PAN fiber (6 g) with DETA (500 g) and through the addition of $AlCl_3{\cdot}6H_2O$ (20 g, Junsei Chemical Co.) at 80–120 °C for various times (30 min to 3 h) with stirring. Excess DETA was used both as a solvent and reactant. The modified PAN fiber, so obtained, was washed with distilled water and ethyl alcohol and then dried at 40 °C *in vacuo*. The synthesis of poly(acrylo-amidino diethylenediamine) is illustrated in Fig. 1.

^{13}C NMR (solid-state): δ = 32.33 (CH_2–CH–C(=NH)–NH–), 35.12 (CH_2–CH–C(=NH)–NH–), 164.61 (CH_2–CH–C(=NH)–NH–), 39.41 (–C(=NH)–NH–CH_2–CH_2–NH–CH_2–CH_2–NH_2), 43.67 (–C(=NH)–NH–CH_2–CH_2–NH–CH_2–CH_2–NH_2), 48.10 (–C(=NH)–NH–CH_2–CH_2–NH–CH_2–CH_2–NH_2), and 36.53 (–C(=NH)–NH–CH_2–CH_2–NH–CH_2–CH_2–NH_2) ppm.

FT-IR (KBr): 3500–2000 (amine group), 1650 (N–C=N, amidine group), 1600 (–NH_2), 1580 (–NH–), and 1481 (CH_2 of diethylenediaimine) cm^{-1}.

Poly(acylo-amidino diethylenediamine) prepared at 120 °C for 3 h was used for the NMR and the FT-IR assignments.

2.2. Measurements

FT-IR spectroscopy (GX FTIR, PerkinElmer) was used to analyze the samples. Samples were cut into approximately 1 mm pieces, blended with KBr, and then pressed into disks for analysis. ^{13}C NMR spectra were obtained on a Bruker MSL200 spectrometer in the solid state. An auto-titrator (716DMS Titrino, Metrohm) was used to get the PADD's equivalent capacity. The quantitative analysis of Cu(II) ions was carried out with atomic absorption spectrophotometry (AAS; SpectrAA 800, Varian). Anions were quantified with ion chromatography (IC; Metrohm); the instrument was fitted with an 762 IC detector, a 709 IC pump, a 752 pump unit, a 733 IC separation center, and a 791 VA detector. The sequential growth of Cu(II) crystals was monitored with FE-SEM (S4200, Hitachi) at 15.0 kV.

2.3. Column experiments

The continuous-flow adsorption experiments were conducted in a PADD fiber packed column with Cu(II) and chromate aqueous solutions. The Cu(II) and chromate aqueous solutions were prepared by dissolving of cupric chloride dehydrate ($CuCl_2{\cdot}2H_2O$, Fluka Chemical Co.) and potassium chromate (K_2CrO_4, Aldrich Chemical Co.) in deionized water, respectively. The used deionized water (DI water, 18.2 MΩ cm^{-1}) was obtained from a Milli-Q water system. The feed solution of 20 L at a known concentration was pumped through the PADD of 60 g packed column using a pump at various flow rates. Sample solutions from the column effluent were collected at regular intervals. The flow rate and pressure of circulated solutions were monitored with a flow meter and pressure sensor. The collected solutions were backed-titrated with an AAS and an IC to calculate the adsorbed amount of metal ions on PADD. The PADD fiber was also collected from the column at regular intervals to observe the adsorption of Cu(II) on them with FE-SEM after drying Cu(II) adsorbed PADD fiber at 40 °C in a vacuum oven.

3. Results and discussion

3.1. Synthesis of poly(acrylo-amidino diethylenediamine) (PADD)

Figs. 2 and 3 show the dominant factors in the synthesis of an amine-containing chelating fiber including reaction time and reaction temperature. It is obvious that the substitution yield of the reaction is consistent with reaction time and temperature. Plots of the adsorption capacity and the substitution yield versus the reaction time of DETA coupling into the PAN fiber at 120 °C are shown in Fig. 2. These plots show curves of S-shape. The reaction is launched above 30 min, and the reaction is significantly accelerated over 90 min. The adsorption capacity and the substitution yield are 11.4 mequiv/g and 97.2%, respectively, at the reaction time of 3 h. The substitution yield is the percentage of the reaction between the nitrile (–C≡N) of PAN and DETA. It was calculated on the basis of elemental analysis (N/C ratio). And the peak of C≡N (nitrile group) was not observed at 2243 cm^{-1} after the reaction.

Fig. 3 shows the adsorption capacity and the substitution yield versus the reaction temperature. All reactions were conducted for 3 h. The substitution yield strongly depended on the reaction

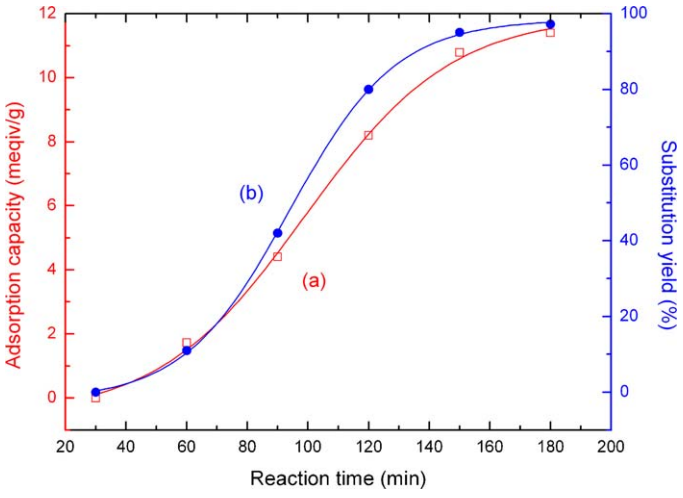

Fig. 2. Substitution yield and adsorption capacity of PADD under reaction times at 120 °C: (a) adsorption capacity and (b) substitution yield.

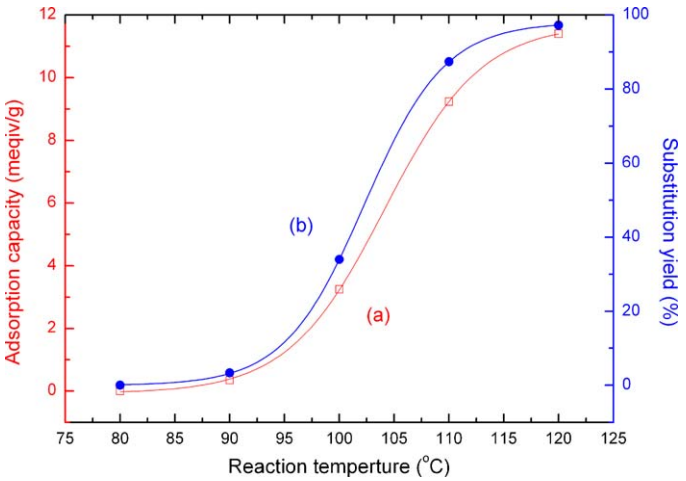

Fig. 3. Substitution yield and adsorption capacity of PADD under reaction temperatures at 3 h: (a) adsorption capacity and (b) substitution yield.

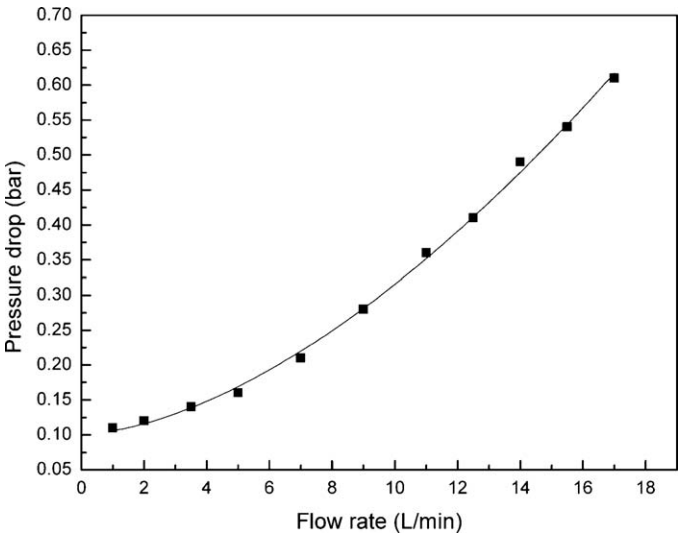

Fig. 5. Pressure drop according to the flow rate in column (adsorption filter cartridge).

temperature as well as time. At 120 °C, 97.2% yield and 11.4 mequiv/g adsorption capacity were accomplished. In these figures, the optimum condition was 3 h at 120 °C for the amination reaction. The reaction was easily controlled by time and temperature. For the following adsorption tests, the chelating fiber (PADD) prepared at the reaction condition of 3 h at 120 °C is used.

3.2. Adsorption of Cu(II) on PADD packed column

Well defined and dried PADD was measured up to 60 g for use of a dynamic test. A column containing 60 g of PADD was assembled and attached to the pump set of designated flow rates. When we use conventional column (vertical direction), the pressure drop was a little high so that effluence was set up in a radial direction to reduce the pressure drop as illustrated in Fig. 4. A packed column is a common, important piece of mass and heat transfer equipment extensively used in chemical process industries, typically in the domain of distillation, absorption, desorption, extraction, etc. [21]. Pressure drop impacts system performance in several ways. The existence of a pressure profile in the axial direction in an adsorption process (both during adsorption and desorption) implies that not all of the adsorbent experiences the full pressure swing available to the system. This directly reduces working capacity [22]. An adopted column in the dynamic test achieved a low-pressure drop as shown in Fig. 5.

20 L of 2, 4, 6, 8, and 10 mM of Cu^{2+} solutions was tested for recycling tests at a rate of 2 L/min as shown in Fig. 6. More than 80% of the copper ion was removed from the 2 mM solution at a fourth cycling. The adsorption amount increased with the increase of the copper ion concentration while the removal efficiency of copper ion decreased. At the fourteenth recycling time, ~100% of the copper ion was removed from the 2 mM solution. However, at the same recycling time, only ~53% of the copper ion was removed from the 10 mM solution.

Fig. 7 demonstrates the effect of the effluent flow rate on the breakthrough curves in removing Cu^{2+} at the concentration of 10 mM. The results indicate that the adsorbed amount of Cu^{2+} on PADD increased with increasing the effluent rate from 1 to 2 L/min.

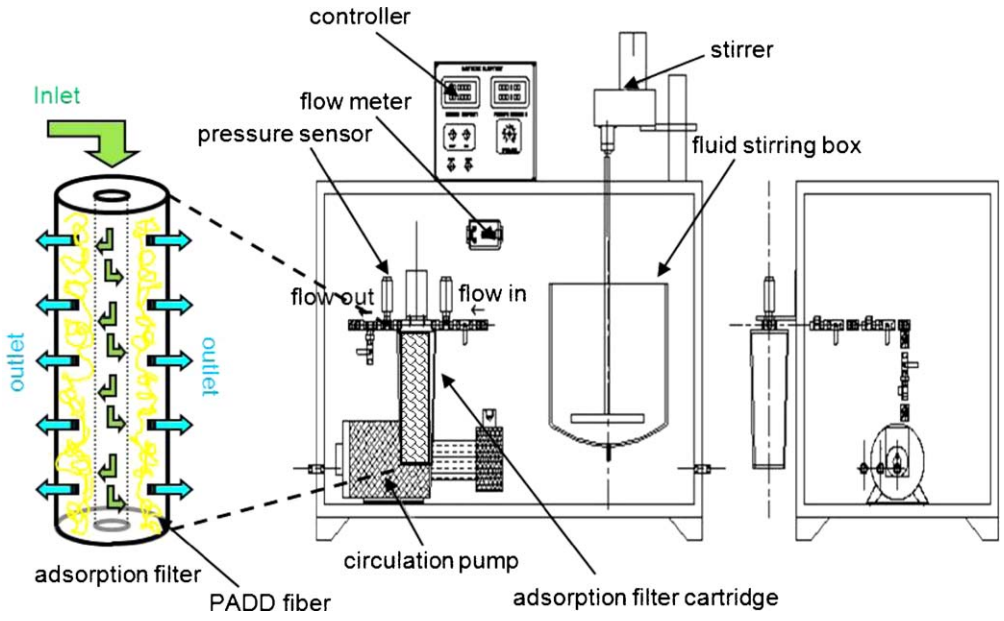

Fig. 4. Schematic presentation of ion exchange system with adsorption filter.

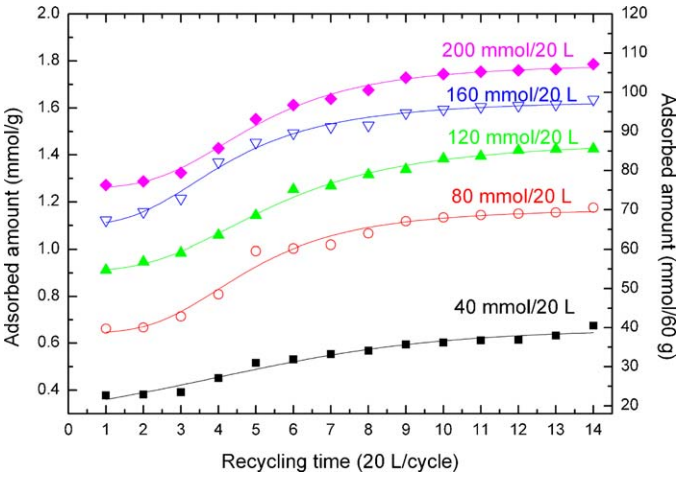

Fig. 6. Adsorption amount of Cu(II) ion in PADD packed column with increase of recycle time at various ion concentrations (flow rate: 2 L/min).

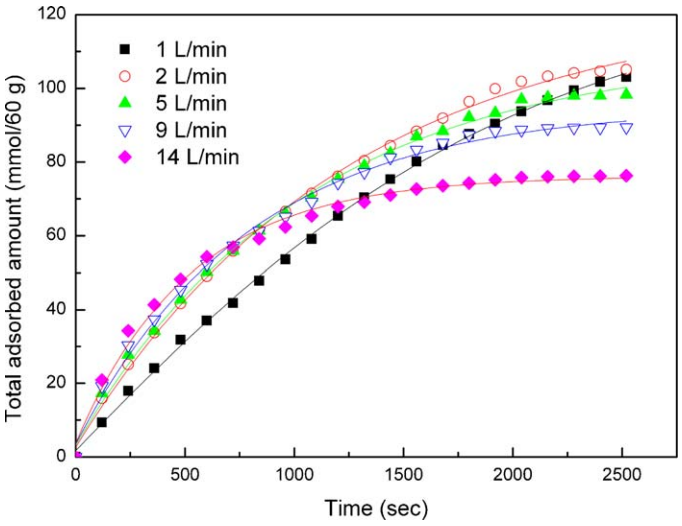

Fig. 7. Adsorption amount of Cu(II) ion in PADD packed column according to the flow time (Cu(II) concentration: 10 mM).

However, the adsorbed amount of Cu^{2+} on PADD decreased with increasing the effluent rate after 2 L/min due to not enough contact times between the Cu^{2+} solution and the PADD packed column. At the initial time for Cu^{2+} adsorption on PADD, adsorbed amount of Cu^{2+} in the high effluent rate is larger than it in the low effluent rate.

The important factor for designing adsorption filter is the uniformly adsorption of the metal ion on whole chelating materials in the filter. The photograph of the filter case is shown in Fig. 8a. The original color of the PADD fiber before Cu^{2+} adsorption is yellow (Fig. 8b). After Cu^{2+} adsorption on the PADD fiber, the color of the fiber changed to light blue (Fig. 8c). We could know that the PADD packed filter was well designed by examining the color of PADD fiber in (Fig. 8d). The whole area of PADD packed filter changed to light blue without the yellow area due to the dead zone of the effluent flow (inset in Fig. 8c).

Interestingly, the crystal growth of copper compounds on PADD was observed during the adsorption process. FE-SEM images of Cu(II) complexes and $Cu(OH)_2$ crystal growth on PADD at various elapsed times (0, 1, 5, 10, 20, and 40 min) are shown in Fig. 9. The adsorption conditions were 2 L/min and 10 mM. The crystal was analyzed with X-ray diffraction (XRD) and X-ray photoelectron (XPS) spectroscopy in our previous work [23]. At the initially elapsed time, $(RNH_3)_2CuCl_4{\cdot}2H_2O$ formed. And after specific time, $Cu(OH)_2$ formed on the PADD fiber. The crystal growth of copper ion on the chelating fiber enhances the adsorption amount. The PADD fiber has its own distinct characteristic of the crystal

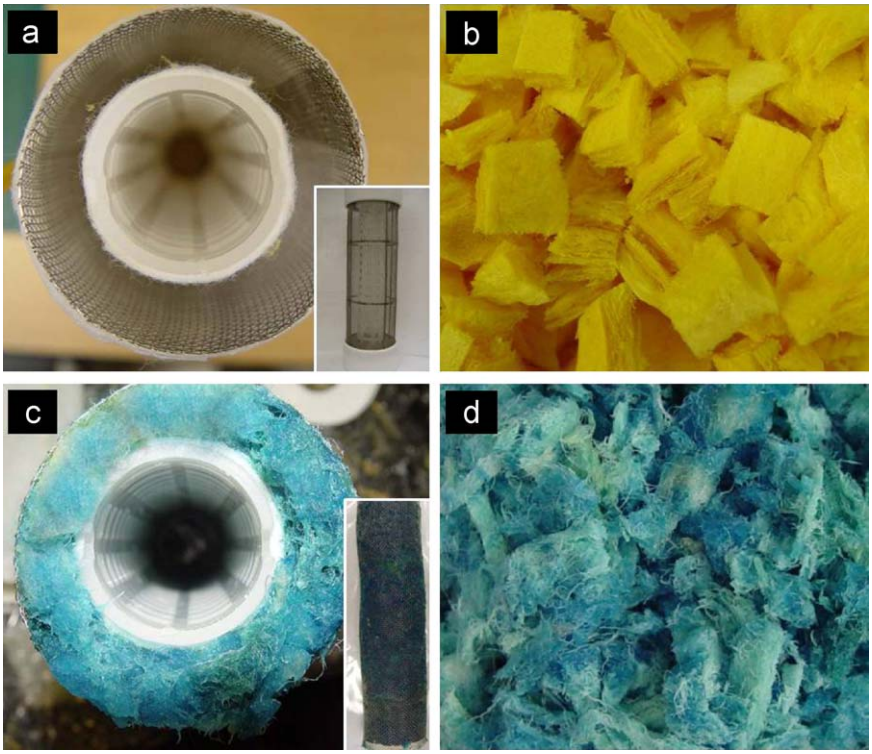

Fig. 8. Photographs of (a) cross-sectional view of empty column (inset: longitudinal view), (b) PADD fiber before adsorption of Cu(II), (c) cross-sectional view of PADD packed column after adsorption of Cu(II) (inset: longitudinal view), and (d) PADD fiber after adsorption of Cu(II).

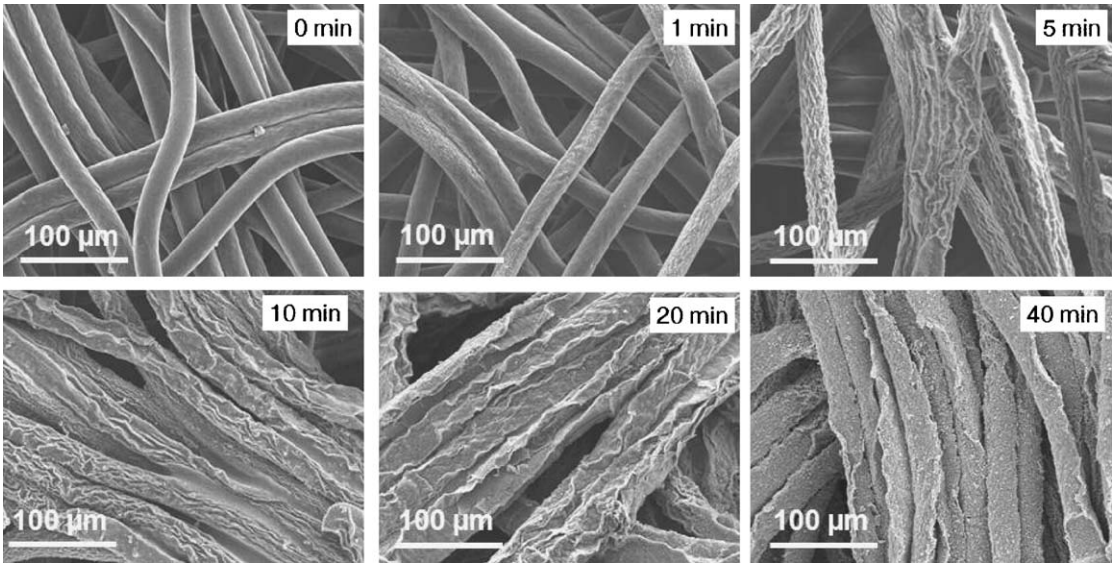

Fig. 9. FE-SEM images of copper crystal growth sequence on PADD (flow rate: 2 L/min, Cu(II) concentration: 10 mM).

growth of metal ions on it which is not observed for other ion exchangers. The PADD packed column showed high performance of removal of Cu(II) in the solution due to the distinct characteristic of PADD.

3.3. Adsorption modeling

Mathematical models can describe the behavior of the adsorption processes operating under different experimental conditions. They are very useful for scaleup studies or process optimizations. A number of models with varying degrees of complexity have been developed to describe the metal adsorption systems [24]. There are of two types: equilibrium and kinetic models.

3.3.1. Equilibrium study (adsorption isotherm)

An adsorption isotherm is used to characterize the interaction of the metal ions with the adsorbents. This provides a relationship between the concentration of metal ions in the solution and the amount of metal ions adsorbed to the solid phase when the two phases are at equilibrium.

To elucidate the adsorption process as a function of the equilibrium concentration in aqueous solutions and to provide better comprehension of the mechanism of adsorption, the following Freundlich isotherm model [25] was considered at constant temperature.

The Langmuir isotherm [26] is the theoretical model for monolayer adsorption onto a surface containing a finite number of identical sites. In this study, the copper ions were adsorbed on the PADD fiber, and formed crystals. Therefore, the Langmuir isotherm cannot be used as a model for Cu^{2+} adsorption on the PADD.

The Freundlich isotherm is an empirical equation which is used to describe adsorption at multilayers and adsorption on a heterogeneous surface.

$$q_e = K_f C_e^{1/n} \quad (1)$$

where q_e (mg/g) is the equilibrium value for removal of adsorbate per unit weight of adsorbent, C_e (mg/L) is the equilibrium concentration of metal ion in solution, and K_f and n are Freundlich isotherm constants which are related to the adsorption capacity (or the bonding energy) and intensity of the sorbent, respectively.

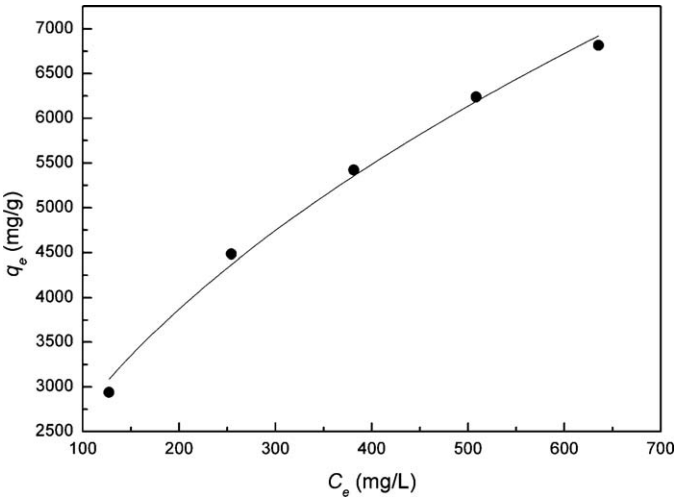

Fig. 10. Experimental data fitting for Cu(II) adsorption into PADD packed column using the Freundlich isotherm.

The adsorption condition is favorable $n > 1$ values. Fig. 10 shows the Freundlich isotherm model plot using experimental data of the equilibrium adsorption. Isotherm parameters of K_f and n calculated from the Freundlich isotherm are 270.64658 and 1.991 with $R^2 = 0.9925$, respectively. The value of 1.991 indicates that Cu^{2+} adsorption on PADD is very favorable. The conformity between experimental data and the model predicted values was expressed by the correlation coefficients (R^2 values close or equal to 1).

3.3.2. Kinetic study

The study of adsorption dynamics describes the solute uptake rate, and this rate controls the habitation time of adsorbate uptake at the solid–solution interface. Chemical kinetics gives information about reaction pathways and times to reach equilibrium. Adsorption kinetics shows a large dependence on the physical and/or chemical characteristics of the sorbent material.

To investigate the mechanism of sorption and the potential rate-controlling steps, the two most widely applied kinetic models were used to fit the experimental data: the pseudo-first-order equation proposed by Lagergren [27] and the pseudo-second-order kinetic

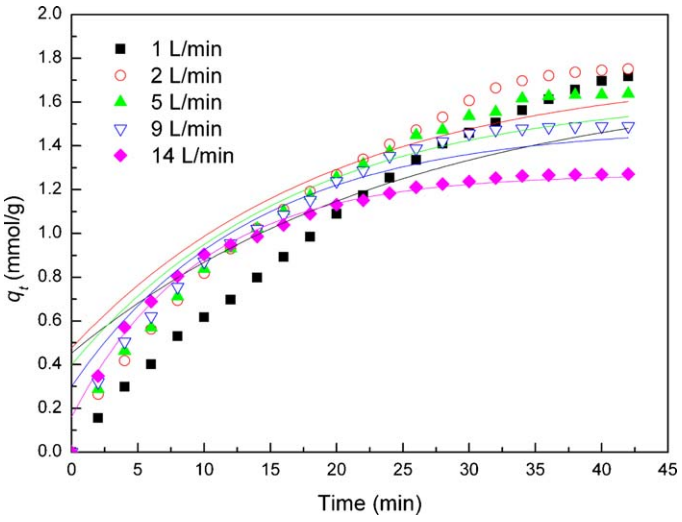

Fig. 11. Fitting of kinetic data for Cu(II) adsorption into PADD packed column using the pseudo-first-order kinetic model.

model proposed by Ho and McKay [28]. The pseudo-first-order and pseudo-second-order equations are given by the following equations, respectively:

$$\log(qe - qt) = \log\, q_e - \frac{k_1 t}{2.303} \quad (2)$$

$$\frac{t}{q_t} = \frac{1}{k_2 q_e^2} + \frac{t}{q_e} \quad (3)$$

where t (min) is the contact time, q_e and q_t (mmol/g) are the amounts of adsorbed Cu^{2+} at equilibrium and time t, and k_1 (min^{-1}) and k_2 (g/mmol min) are the rate constants of the pseudo-first-order and pseudo-second-order kinetics, respectively [29]. Figs. 11 and 12 show the pseudo-first-order and pseudo-second-order kinetics model plots using experimental data from Fig. 7. It can be concluded that the pseudo-first-order equation is the model that best describes the experimental data at the initial time while pseudo-second-order model describes the experimental data at the near equilibrium time. It is thought that the optimum kinetics model depends on the time because Cu^{2+} adsorbs on the PADD fiber as the ion form at the initial time and forms the $Cu(OH)_2$ crystal

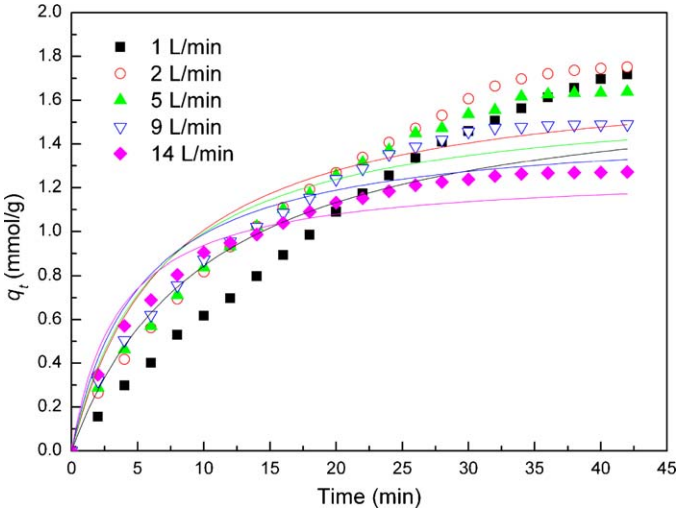

Fig. 12. Fitting of kinetic data for Cu(II) adsorption into PADD packed column using the pseudo-second-order kinetic model.

Table 1
Kinetic parameters for adsorption of Cu(II) on chelating fiber at different flow rates.

Flow rate (L/min)	Pseudo-first-order model		Pseudo-second-order model	
	k_1 (min^{-1})	R^2	k_2 (g/mmol min)	R^2
1	0.09176	0.81242	0.0563	0.85132
2	0.11789	0.86623	0.0771	0.87735
5	0.13543	0.90556	0.09439	0.88609
9	0.17116	0.94711	0.13242	0.89597
14	0.24317	0.98647	0.22042	0.93699

on the fiber after its adsorption on the fiber. Therefore, two different kinetics models are required to obtain the good fitting for these two different adsorptions. On the basis of the above two kinetic models, the obtained parameters for the adsorption kinetics are summarized in Table 1.

3.4. Adsorption of chromate ion on PADD packed column

Fig. 13 shows recycling adsorption tests at a rate of 2 L/min for 20 L of 2, 6, and 10 mM of CrO_4^{2-} solutions. More than 80% of the chromate ion was removed from the 2 mM solution at a ninth cycling. The adsorption amount increased with the increase of the chromate ion concentration while the removal efficiency of chromate ion decreased. At the fourteenth recycling time, ~100% of the CrO_4^{2-} was removed from the 2 mM solution. After CrO_4^{2-} adsorption on the PADD fiber, the color of the fiber changed to dark yellow (inset in Fig. 13).

Fig. 14 demonstrates the effect of the effluent flow rate on the breakthrough curves in removing CrO_4^{2-} at the concentration of 10 mM. The results indicate that the adsorbed amount of CrO_4^{2-} on PADD increased with increasing the effluent rate from 1 to 5 L/min. However, the adsorbed amount of CrO_4^{2-} on PADD decreased with increasing the effluent rate after 5 L/min due to not enough contact times between the CrO_4^{2-} solution and the PADD packed column. At the initial time for CrO_4^{2-} adsorption on PADD, adsorbed amount of CrO_4^{2-} in the high effluent rate is larger than it in the low effluent rate. The tendency of the CrO_4^{2-} adsorption on the effluent rate was same with the Cu^{2+} adsorption.

Fig. 15 shows the Freundlich isotherm model plot using experimental data of the equilibrium adsorption. Isotherm parameters of K_f and n calculated from the Freundlich isotherm are 271.07583 and 1.901 with $R^2 = 0.9890$, respectively. The value of 1.901 indicates that CrO_4^{2-} adsorption on PADD is very favorable.

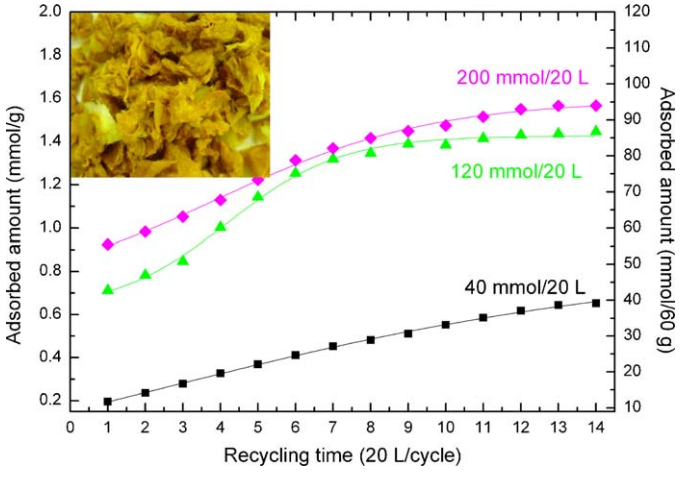

Fig. 13. Adsorption amount of chromate ion in PADD packed column with increase of recycle time at various ion concentrations (flow rate: 2 L/min).

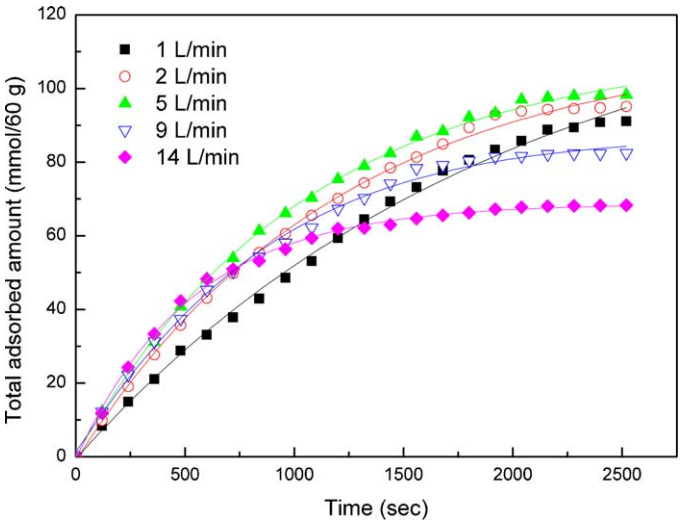

Fig. 14. Adsorption amount of chromate ion in PADD packed column according to the flow time (chromate ion concentration: 10 mM).

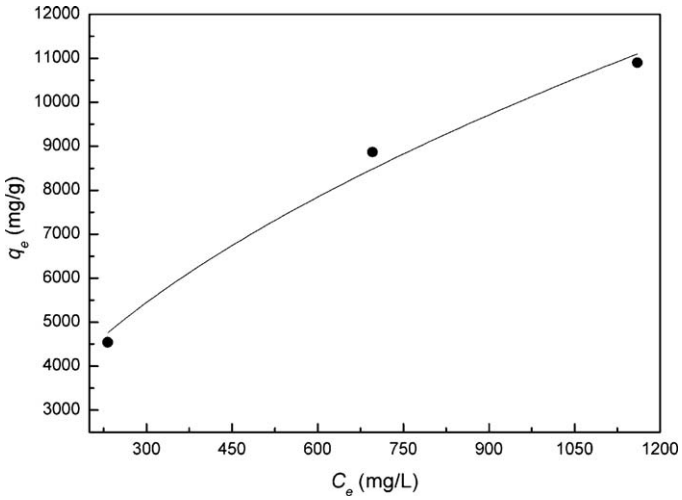

Fig. 15. Experimental data fitting for chromate ion adsorption into PADD packed column using the Freundlich isotherm.

4. Conclusions

As a chelating fiber, PADD was synthesized by the coupling of the PAN fiber with diethylenetriamine under catalyst, $AlCl_3{\cdot}6H_2O$. The optimum conditions for the amination were 3 h at 120 °C. The maximum removal capacity and substitution yield were 11.4 mequiv/g and 97.2%. The Cu^{2+} and CrO_4^{2-} adsorption process in the flow test was finished at the about 2520 s with the 60 g of PADD packed column. More than 80% of the copper ion was removed from the 2 mM solution at a fourth cycling. The adsorption amount increased with the increase of the copper ion concentration while the removal efficiency of copper ion decreased. At the fourteenth recycling time, ~100% of the copper ion was removed from the 2 mM solution. Interestingly, the crystal growth of copper compounds on PADD was observed during the adsorption process. The PADD packed column showed high performance of removal of Cu^{2+} in the solution due to the distinct characteristic of the crystal growth of metal ions on PADD. Isotherm parameters of K_f and n calculated from the Freundlich isotherm equation for the adsorption equilibrium data are 270.64658 and 1.991 with $R^2 = 0.9925$, respectively. The value of 1.991 indicates that Cu^{2+} adsorption on PADD is very favorable. At the kinetic study, it can be concluded with model plots using experimental data that the pseudo-first-order equation is the model that best describes the experimental data at the initial time while pseudo-second-order model describes the experimental data at the near equilibrium time because of the $(CuOH)_2$ crystals growth after Cu^{2+} ion adsorption on the PADD fiber. The PADD packed column showed also high performance of removal of Cr(VI) in the solution. We expect that the use of the chelating fiber, which can grow the crystal of metal ions onto it, surpasses the removal limit of metal ions for the established ion exchange system in the aqueous solution.

References

[1] P.C. Nagajyoti, K.D. Lee, T.V.M. Sreekanth, Heavy metals, occurrence and toxicity for plants: a review, Environ. Chem. Lett. 8 (2010) 199–216.
[2] F. Rashidi, R.S. Sarabi, Z. Ghasemi, A. Seif, Kinetic equilibrium and thermodynamic studies for the removal of lead(II) and copper(II) ions from aqueous solutions by nanocrystalline TiO_2, Superlattices Microstruct. 48 (2010) 577–591.
[3] J. Lee, S. Mahendra, P.J.J. Alvarez, Nanomaterials in the construction industry: a review of their applications and environmental health and safety considerations, ACS Nano 4 (2010) 3580–3590.
[4] A. Hosseini-Bandegharaei, M.S. Hosseini, M. Sarw-Ghadi, S. Zowghi, E. Hosseini, H. Hosseini-Bandegharaei, Kinetics equilibrium and thermodynamic study of Cr(VI) sorption into toluidine blue o-impregnated XAD-7 resin beads and its application for the treatment of wastewaters containing Cr(VI), Chem. Eng. J. 160 (2010) 190–198.
[5] M. Kashiwa, S. Nishimoto, K. Takahashi, M. Ike, M. Fhjita, Factors affecting soluble selenium removal by a selenate-reducing bacterium Bacillus sp. SF-1, J. Biosci. Bioeng. 89 (2000) 528–533.
[6] F. Ma, R. Qu, C. Sun, C. Wang, C. Ji, Y. Zhang, P. Yin, Adsorption behaviors of Hg(II) on chitosan functionalized by amino-terminated hyperbranched polyamidoamine polymers, J. Hazard. Mater. 172 (2009) 792–801.
[7] Y.G. Ko, U.S. Choi, J.S. Kim, Y.S. Park, Novel synthesis and characterization of activated carbon fiber and dye adsorption modeling, Carbon 40 (2002) 2661–2672.
[8] S.M. Kraemer, J.D. Xu, K.N. Raymond, G. Sposito, Adsorption of Pb(II) and Eu(III) by oxide minerals in the presence of natural and synthetic hydroxamate siderophores, Environ. Sci. Technol. 36 (2002) 1287–1291.
[9] J.P. Chen, L.A. Hong, S.N. Wu, L. Wang, Elucidation of interactions between metal ions and Ca alginate-based ion-exchange resin by spectroscopic analysis and modeling simulation, Langmuir 18 (2002) 9413–9421.
[10] J. Kostal, A. Mulchandani, W. Chen, Tunable biopolymers for heavy metal removal, Macromolecules 34 (2001) 2257–2261.
[11] M.G. Hankins, T. Hayashita, S.P. Kasprzyk, R.A. Bartsch, Immobilization of crown ether carboxylic acids on silica gel and their use in column concentration of alkali metal cations from dilute aqueous solutions, Anal. Chem. 68 (1996) 2811–2817.
[12] A.C. Templeton, F.P. Zamborini, W.P. wuelfing, R.W. Murray, Controlled and reversible formation of nanoparticle aggregates and films using Cu^{2+}-carboxylate chemistry, Langmuir 16 (2000) 6682–6688.
[13] B.L. Westcott, N.E. Gruhn, J.H. Enemark, Evaluation of molybdenum–sulfur interactions in molybdoenzyme model complexes by gas-phase photoelectron spectroscopy. The electronic buffer effect, J. Am. Chem. Soc. 120 (1998) 3382–3386.
[14] J.E. McCusker, K.A. Abboud, L. McElwee-White, Carbonylation of amines with a tungsten(IV) carbonyl complex, Organometallics 16 (1997) 3863–3866.
[15] U.S. Schubert, C. Eschbaumer, Macromolecules containing bipyridine and terpyridine metal complexes: towards metallosupramolecular polymers, Angew. Chem. Int. Ed. 41 (2002) 2893–2926.
[16] B. Wrackmeyer, Metal complexes bearing terminal borylene ligands, Angew. Chem. Int. Ed. 38 (1999) 771–772.
[17] D. Jermakowicz-Bartkowiak, B.N. Kolarz, Poly(4-vinylpyridine) resins towards perrhenate sorption and desorption, React. Funct. Polym. 71 (2011) 95–103.
[18] N. Ma, Y. Yang, S. Chen, Q. Zhang, Preparation of amine group-containing chelating fiber for through removal of mercury ions, J. Hazard. Mater. 171 (2009) 288–293.
[19] P.K. Neghlani, M. Rafizadeh, F.A. Taromi, Preparation of aminated-polyacrylonitrile nanofiber membranes for the adsorption of metal ions: comparison with microfibers, J. Hazard. Mater. 186 (2011) 182–189.
[20] Y.G. Ko, U.S. Choi, Y.S. Park, J.W. Woo, Fourier transform infrared spectroscopy study of the effect of pH on anion and cation adsorption onto poly(acryloamidinodiethylenediamine), J. Polym. Sci. Part A: Polym. Chem. 42 (2004) 2010–2018.
[21] G.Q. Wang, X.G. Yuan, K.T. Yu, Review of mass-transfer correlations for packed columns, Ind. Eng. Chem. Res. 44 (2005) 8715–8729.
[22] F. Rezaei, P. Webley, Structured adsorbents in gas separation processes, Sep. Purif. Technol. 70 (2010) 243–256.
[23] Y.G. Ko, D.H. Shin, U.S. Choi, Pinecone-like Cu(II) crystal growth on the surface of amine-group-immobilized polymers, J. Polym. Sci. Part A: Polym. Chem. 43 (2005) 1238–1247.
[24] B. Saha, C. Orvig, Biosorbents for hexavalent chromium elimination from industrial and municipal effluents, Coord. Chem. Rev. 254 (2010) 2959–2972.

[25] H. Freundlich, W. Heller, The adsorption of cis- and trans-azobenzene, J. Am. Chem. Soc. 61 (1939) 2228–2230.
[26] I. Langmuir, Chemical reaction at low pressure, J. Am. Chem. Soc. 37 (1915) 1139–1167.
[27] S. Lagergren, About the theory of so-called adsorption of soluble substances, K. Sven. Vetenskapsakad. Handl. 24 (1898) 1–39.
[28] Y.S. Ho, G. McKay, Pseudo-second order model for sorption processes, Process Biochem. 34 (1999) 451–465.
[29] S. Lazarević, I. Janković-Častvan, V. Djokić, Z. Radovanović, D. Janaćković, R. Petrović, Iron-modified sepiolite for Ni^{2+} sorption from aqueous solution: an equilibrium, kinetic, and thermodynamic study, J. Chem. Eng. Data 55 (2010) 5681–5689.